



## Simulation of fresh concrete slump test with the Material Point Method

Leonardo T. Ferreira<sup>1</sup>, Tiago P. S. Lôbo<sup>1</sup>, Ricardo A. Fernandes<sup>1</sup>, Lucas G. O. Lopes<sup>1</sup>, Lorrán F. Oliveira<sup>1</sup>, Luciana C. L. M. Vieira<sup>2</sup>, Adeildo S. Ramos Jr<sup>2</sup>

<sup>1</sup>Laboratory of Scientific Computing and Visualization, Federal University of Alagoas

Campus A.C. Simões - Av. Lourival Melo Mota, without number, Tabuleiro do Martins, 57072-970, Maceió/Alagoas, Brazil

leonardotoledo@lccv.ufal.br, tiago@lccv.ufal.br, ricardoaf@lccv.ufal.br, lucas.omena@lccv.ufal.br, lorrán.oliveira@lccv.ufal.br  
<sup>2</sup>Dept. of Structures, Federal University of Alagoas

Campus A.C. Simões - Av. Lourival Melo Mota, without number, Tabuleiro do Martins, 57072-970, Maceió/Alagoas, Brazil

lucianaclmv@lccv.ufal.br, adramos@lccv.ufal.br

**Abstract.** The exponential growth in computational power in recent years has increasingly made numerical simulations a go-to tool for studying the behavior of structures and materials. A pertinent application is the simulation of the fresh concrete slump test, a laboratory test used to study the consistency and mobility of the concrete mixture. However, this simulation presents a challenge, as concrete — composed of a varied mixture of materials like water, cement, sand, and gravel — exhibits viscoplastic behavior. Therefore, a robust numerical method that models this physical nonlinearity is necessary. Previous works have successfully simulated the fresh concrete slump test as a Herschel-Bulkley fluid, utilizing the lattice Boltzmann method. Meanwhile, the Generalized Interpolation Material Point (GIMP) method is gaining traction in the industry. GIMP unites the best traits of mesh-based methods with the best traits of particle-based methods, by combining a fixed background grid of finite elements (i.e., a grid that remains still throughout the simulation) with material points where the kinematic data is stored. This approach favors the simulation of large displacements and deformations. In this work, GIMP is adopted to numerically simulate the fresh concrete slump test with the Herschel-Bulkley model.

**Keywords:** Slump test, Herschel-Bulkley, Numerical simulation, Nonlinear behavior, Material Point Method

## 1 Introduction

The slump test is used in the industry to evaluate the workability and flowability of fresh concrete. The test is performed by filling a standard mold (Figure 1) with the fresh concrete mixture. The mold is then removed and the mixture flows. From the observation of the flow, it can be determined if the mixture needs more water or additives, depending on the desired use case for the concrete.

To numerically simulate this test, a model for the behavior of the fresh concrete mixture is necessary. Academic research suggests that the Herschel-Bulkley rheological model is a viable option for describing the flow of fresh concrete, as its constitutive equation follows the fresh concrete behavior more closely than the Bingham model (De Larrard et al. [1], Hemphill et al. [2]).

Furthermore, a numerical method is necessary for the discretization of the physical domain (Figure 2). In this work, the Generalized Interpolation Material Point (GIMP) method is adopted. This method was developed as an extension of the original Material Point Method (Sulsky et al. [3]). MPM has already been successfully used in the simulation of many challenging problems, such as anchor modelling (Coetzee et al. [4]), runoff of landslides (Andersen and Andersen [5]), impact in general (Chen et al. [6]), collapse of granular columns (Mast et al. [7]), avalanches (Mast et al. [8]), hydromechanics (Abe et al. [9]), impact of submarine landslides (Dong et al. [10]), and slope stability (Wang [11]).

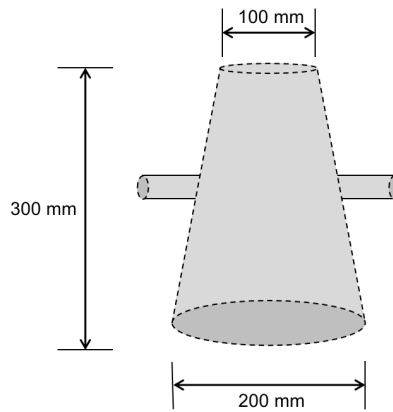


Figure 1. Representation of the cone-shaped trunk used as a mold for the slump test of fresh concrete. Before the test, the mold must be filled to the top with a fresh concrete mixture and any excessive material is removed. During the test, the operator must pull firmly on the handles to move the mold upwards so that the concrete may flow .

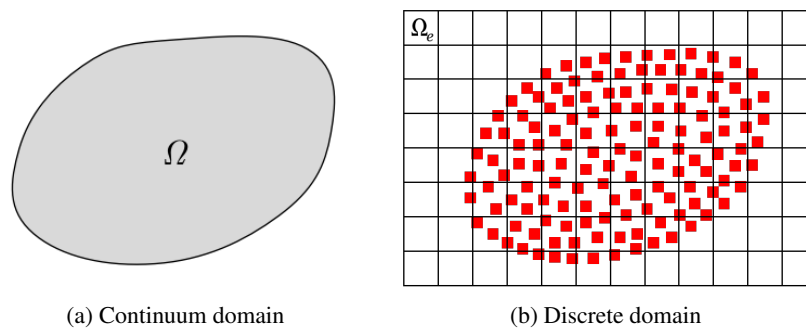


Figure 2. Discretization of the physical domain in GIMP. In this method, the continuum domain (a) is represented by a set of material points (or particles), represented in the color red (b). Alongside the particles, a fixed background grid is created. As the background grid remains still during the simulation, it must cover the entire region that the particles may occupy.

GIMP unites the best traits of mesh-based methods with the best traits of particle-based methods, by adopting a fixed background grid of finite elements (i.e., a grid that remains still throughout the simulation) alongside the material points where kinematic data (such as displacement, velocity, and acceleration) is stored. During a typical GIMP time step (Figure 3), data is transferred between the particles and the background grid. In summary, particle data is mapped to the background grid, where the equations of motion are solved. Then, the results are mapped back from the grid to the particles. Finally, an update of particle kinematics is performed.

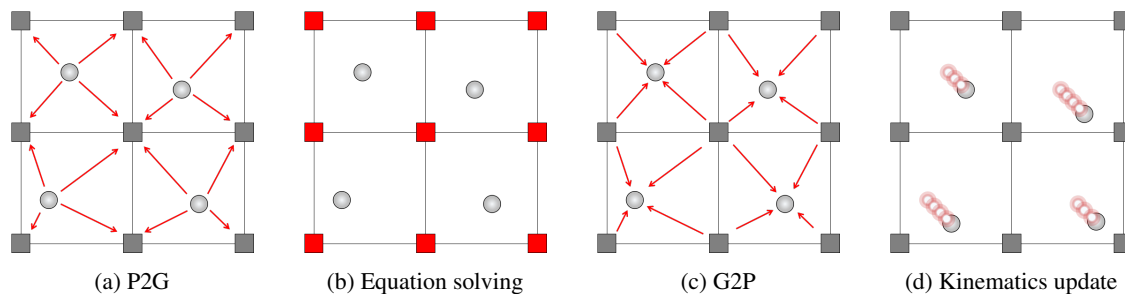


Figure 3. The four basic steps in a typical GIMP time step. a) Particle data is mapped to the background grid (P2G). b) The equations of motion are solved in the background grid. c) Grid results are mapped back to the particles. d) Update of particle kinematics with the mapped results.

## 2 Formulation

In this section, a brief discussion of the mathematical aspects of the numerical method (GIMP) and the constitutive equation is realized.

### 2.1 Generalized Interpolation Material Point Method (GIMP)

GIMP is built upon the variational form for conservation of momentum:

$$\int_{\Omega} \rho \mathbf{a} \cdot \delta \mathbf{v} \, d\mathbf{x} + \int_{\Omega} \boldsymbol{\sigma} : \nabla \delta \mathbf{v} \, d\mathbf{x} = \int_{\Omega} \rho \mathbf{b} \cdot \delta \mathbf{v} \, d\mathbf{x}, \quad (1)$$

in which:

$\Omega$ : current volume,

$\rho$ : mass density,

$\mathbf{a}$ : acceleration,

$\delta \mathbf{v}$ : admissible velocities,

$\mathbf{x}$ : current position,

$\boldsymbol{\sigma}$ : Cauchy stress,

$\mathbf{b}$ : specific body force.

By introducing a particle characteristic function  $\chi_p^i(\mathbf{x})$ , which is a partition of unity, and by defining the initial particle volume as  $V_p^i = \int_{\Omega^i} \chi_p^i(\mathbf{x}) \, d\mathbf{x}$ , in which  $\Omega^i$  is the initial volume of the continuum body, the discretization procedure takes course. In particular, this work adopts the Contiguous Particle GIMP Method, i.e. the particle characteristic function is chosen to guarantee that there is no overlap among particle volumes (Bardenhagen et al. [12]). In this scenario, the particles are represented as rectangles with a side length of  $2l_p$ . A set of weighting functions  $\bar{N}_{np}$  and gradient weighting functions  $\bar{\nabla} N_{np}$  cover the interface between the particles and the nodes:

$$\bar{N}_{np} = \frac{1}{2l_p} \int_{x_p-l_p}^{x_p+l_p} N_n(x) \, dx, \quad (2)$$

$$\bar{\nabla} N_{np} = \frac{1}{2l_p} \int_{x_p-l_p}^{x_p+l_p} \nabla N_n(x) \, dx, \quad (3)$$

in which  $x_p$  is the particle position,  $N_n(x)$  is the nodal shape function and  $\nabla N_n(x)$  the gradient nodal shape function.

In this setting, the equation of motion is written as:

$$\dot{\mathbf{p}}_n = \mathbf{f}_n^{ext} - \mathbf{f}_n^{int}, \quad (4)$$

in which:

$\dot{\mathbf{p}}_n = \sum_p \dot{\mathbf{p}}_p \bar{N}_{np}$ : nodal momentum (in terms of the particle momentum  $\dot{\mathbf{p}}_p$  and the weighting function  $\bar{N}_{np}$ ),

$\mathbf{f}_n^{ext} = \sum_p m_p \mathbf{g} \bar{N}_{np}$ : external nodal force or self-weight (in terms of the particle mass  $m_p$  and the gravitational acceleration  $\mathbf{g}$ ),

$\mathbf{f}_n^{int} = \sum_p V_p \boldsymbol{\sigma}_p \cdot \bar{\nabla} N_{np}$ : internal nodal force (in terms of the particle volume  $V_p$ , the particle stress  $\boldsymbol{\sigma}_p$  and the gradient weighting function  $\bar{\nabla} N_{np}$ ).

This work adopts the Euler method (an explicit time integration scheme). Thus, a critical value of the time step ( $\Delta t_{critical}$ ) is defined (the user-defined time step may be a fraction of this critical time step, but never by bigger than it):

$$\Delta t_{critical} = \frac{\Delta x}{c}, \quad (5)$$

in which,

$\Delta x$ : element size on the fixed background grid,

$c$ : sound wave propagation speed in the material.

Since the internal nodal forces depend on particle stresses, the moment on which stresses are updated, i.e., before or after solving the equation of motion in a given time step, leads to different results. Two commonly adopted approaches are the *Update Stresses Last* (USL) and *Update Stresses First* (USF) algorithms. In USF, the stress update step is performed after mapping the G2P step. Conversely, in USL the stress update step is performed before the G2P step. USF is a conservative algorithm, but can lead to an overall increase of the energy level in system (Bardenhagen [13]). Therefore, this article adopts USL.

## 2.2 Constitutive equation

For the computation of the Cauchy stress tensor, the fluid constitutive equation is used (Batchelor [14]):

$$\boldsymbol{\sigma} = -p\mathbf{I} + 2\mu \left( \mathbf{D} - \frac{1}{3}\text{tr}(\mathbf{I}) \right), \quad (6)$$

in which:

- $p$ : fluid pressure,
- $\mathbf{I}$ : identity matrix,
- $\mu$ : fluid viscosity,
- $\mathbf{D}$ : strain rate tensor,
- tr: trace operator.

The Herschel-Bulkley model is introduced to the constitutive equation by replacing the viscosity  $\mu$  by the apparent viscosity  $\mu_{ap}$ , which, for this model, is given by (Li et al. [15]):

$$\mu_{ap} = \frac{s_{u0}}{\dot{\gamma}} \left( 1 - e^{-m|\dot{\gamma}|} \right) + k\dot{\gamma}^{n-1}, \quad (7)$$

in which:

- $s_{u0}$ : initial undrained shear strength,
- $\dot{\gamma}$ : local shear rate, given by  $\dot{\gamma} = \sqrt{2|\mathbf{D}|}$ , in which  $|\mathbf{D}|$  is the squared norm of the shear strain rate,
- $m$ : regularization parameter,
- $k$ : consistency index,
- $n$ : power-law index.

## 3 Slump test simulation

A computational model of the slump test was developed (Figure 4). In the model, a trunk-shaped cone of particles (with standard dimensions, i.e. a bottom diameter of 200 mm, and a top diameter of 100 mm) is subjected to the acceleration of gravity, under a background grid of hexahedral elements. The nodes at the bottom face of the grid are locked in the vertical direction to prevent the particles from escaping the grid. As the position of the nodes remains the same over time, the grid must cover the entire region that the particles may occupy throughout the simulation. The numerical model parameters (Table 1) were selected to find a middle ground between performance and precision. The fresh concrete is modeled as a Herschel-Bulkley fluid (Table 2), with the same parameters as the group G3 concrete from Li et al. [15].

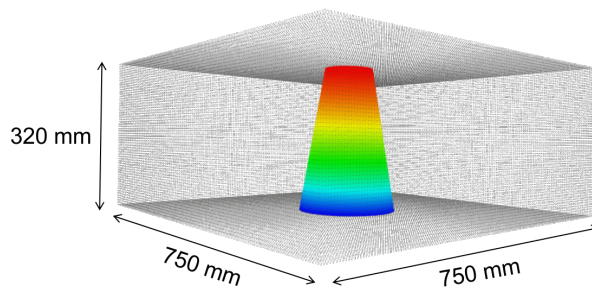


Figure 4. Computational model of the slump test.

Table 1. Numerical model parameters

Parameter	Value
Background grid element size	0.005 m
Number of elements	1,247,389
Number of nodes	1,364,224
Number of particles	351,860
Gravitational acceleration	9.81 m/s <sup>2</sup>
Percentage of the critical time step	25%
Simulation time	4 s

Table 2. Fresh concrete material parameters from the Herschel-Bulkley fluid model

Parameter	Value
Mass density ( $\rho$ )	2574 kg/m <sup>3</sup>
Initial undrained shear strength ( $s_{u0}$ )	188.91 Pa
Consistency index ( $k$ )	45.65 Pa·s <sup><math>n</math></sup>
Power-law index ( $n$ )	1.33
Regularization parameter ( $m$ )	1000

As the Herschel-Bulkley material (an incompressible fluid) is approximated by a compressible fluid with low compressibility, the sound speed in the fluid ( $c$ ) must be of a high enough value to ensure that compressibility effects are negligible. In this simulation,  $c$  was approximated by  $50\sqrt{2gh}$ , in which  $g$  is the gravitational acceleration and  $h$  is the height of the trunk-shaped cone.

#### 4 Results and discussion

In the slump test simulation (Figure 5), there is a visually pronounced initial deformation of the fresh concrete mixture, succeeded by a gradual and continuous flow. Specifically, at time  $t = 0$  s, the concrete maintains the shape of the mold, i.e. a trunk-shaped cone. As time progresses to  $t = 0.1$  s and  $t = 0.2$  s, the concrete demonstrates signs of flow, albeit while largely retaining its initial contour. By  $t = 0.5$  s, the concrete exhibits a markedly dissimilar shape, manifesting a disc-like morphology. Finally, at  $t = 3$  s, the flow has predominantly stabilized, and any resemblance to the initial shape of the fresh concrete has been entirely lost.

Numerically, it was observed that the time necessary for reaching a diameter of 500 mm ( $T_{500}$ ) was 3.8 s. In the basis work (Li et al. [15]), the value of  $T_{500}$  was 3.5 s, giving a relative error of approximately 9%. This result is deemed satisfactory, considering that the reference work uses the lattice Boltzmann method, with a completely different numerical formulation.

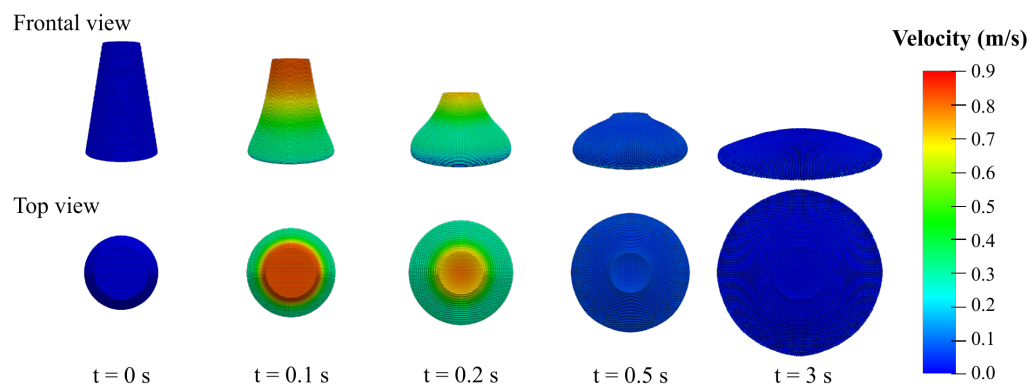


Figure 5. Flow of fresh concrete under no-slip condition in the slump test model.

## 5 Conclusions

The Generalized Interpolation Material Point Method proved to be capable of handling the slump test simulation, as the results are consistent with Li et al. [15]. Better GIMP results are to be expected with a more refined model, i.e. an increase in the number of particles and a finer background grid. It is important, however, to balance the quality of the results with the performance cost of the simulation, as a more refined model might present a computational cost that does not justify its uptick in quality.

**Acknowledgements.** This work was partially funded by the National Council for Scientific and Technological Development (CNPq) and Petróleo Brasileiro S.A. (Petrobras).

**Authorship statement.** The authors hereby confirm that they are the sole liable persons responsible for the authorship of this work, and that all material that has been herein included as part of the present paper is either the property (and authorship) of the authors, or has the permission of the owners to be included here.

## References

- [1] F. De Larrard, C. Ferraris, and T. Sedran. Fresh concrete: a herschel-bulkley material. *Materials and structures*, vol. 31, n. 7, pp. 494–498, 1998.
- [2] T. Hemphill, W. Campos, and A. Pilehvari. Yield-power law model more accurately predicts mud rheology. *Oil and Gas Journal; (United States)*, vol. 91:34, 1993.
- [3] D. Sulsky, Z. Chen, and H. L. Schreyer. A particle method for history-dependent materials. *Computer Methods in Applied Mechanics and Engineering*, vol. 118, pp. 179–196, 1994.
- [4] C. J. Coetzee, P. A. Vermeer, and A. H. Basson. The modelling of anchors using the material point method. *International Journal for Numerical and Analytical Methods in Geomechanics*, vol. 29, n. 9, pp. 879–895, 2005.
- [5] S. M. Andersen and L. V. Andersen. Modelling of landslides with the material-point method. *Computational Geosciences*, vol. 14, n. 1, pp. 137–147, 2010.
- [6] Z. Chen, Y. Han, S. Jiang, Y. Gan, and T. D. Sewell. A multiscale material point method for impact simulation. *Theoretical and Applied Mechanics Letters*, vol. 2, n. 5, pp. 051003, 2012.
- [7] C. M. Mast, P. Arduino, P. Mackenzie-Helnwein, and G. R. Miller. Simulating granular column collapse using the Material Point Method. *Acta Geotechnica*, vol. 10, n. 1, pp. 101–116, 2014a.
- [8] C. M. Mast, P. Arduino, G. R. Miller, and P. Mackenzie-Helnwein. Avalanche and landslide simulation using the material point method: flow dynamics and force interaction with structures. *Computational Geosciences*, vol. 18, n. 5, pp. 817–830, 2014b.
- [9] K. Abe, K. Soga, and S. Bandara. Material Point Method for Coupled Hydromechanical Problems. *Journal of Geotechnical and Geoenvironmental Engineering*, vol. 140, n. 3, pp. 04013033, 2014.
- [10] Y. Dong, D. Wang, and M. F. Randolph. Investigation of impact forces on pipeline by submarine landslide using material point method. *Ocean Engineering*, vol. 146, pp. 21–28, 2017.
- [11] B. Wang. *Slope failure analysis using the material point method*. PhD thesis, TU Delft University of Technology, 2017.
- [12] S. G. Bardenhagen, E. M. Kober, and others. The generalized interpolation material point method. *Computer Modeling in Engineering and Sciences*, vol. 5, n. 6, pp. 477–496, 2004.
- [13] S. G. Bardenhagen. Energy conservation error in the material point method for solid mechanics. *Journal of Computational Physics*, vol. 180, n. 1, pp. 383–403, 2002.
- [14] G. K. Batchelor. *An Introduction to Fluid Dynamics*. Cambridge University Press, 1 edition, 2000.
- [15] Y. Li, J. Mu, Z. Wang, Y. Liu, and H. Du. Numerical simulation on slump test of fresh concrete based on lattice boltzmann method. *Cement and Concrete Composites*, vol. 122, pp. 104136, 2021.